Polymer Chemistry

ROYAL SOCIETY OF CHEMISTRY

PAPER

View Article Online
View Journal | View Issue

Cite this: *Polym. Chem.*, 2023, **14**, 587

Thermo- and pH-responsive poly[(diethylene glycol methyl ether methacrylate)-*co*-(2-diisopropylamino ethyl methacrylate)] hyperbranched copolymers: self-assembly and drug-loading†

Dimitrios Selianitis and Stergios Pispas *

We present the synthesis of a new series of thermo- and pH-responsive poly[(diethylene glycol methyl ether methacrylate)-*co*-(2-diisopropylamino ethyl methacrylate)], P(DEGMA-*co*-DIPAEMA), hyperbranched copolymers and studies regarding their self-assembly in aqueous media. Three P(DEGMA-*co*-DIPAEMA) hyperbranched copolymers, with different ratios of hydrophobic to hydrophilic segments, are synthesized *via* reversible addition–fragmentation chain transfer (RAFT) polymerization using the branching agent ethylene glycol dimethacrylate (EGDMA). By employing several physicochemical characterization techniques, it was possible to determine the properties of self-assembled nanostructures, which are responsive to changes in aqueous solution temperature and pH. Dynamic light scattering (DLS) verified the formation of nano-aggregates in aqueous media, in particular at pH 3 and at both low and high temperatures (25 °C, 55 °C), where all hyperbranched copolymers form the largest aggregates compared to the other two pH conditions investigated (*i.e.*, pH 7 and pH 10). In addition, the hyperbranched copolymers were able to encapsulate the hydrophobic drug indomethacin (IND) at different loading ratios. IND release experiments were performed at pH 7, and revealed that a high amount of the entrapped IND is strongly attached to the hydrophobic domains of the hyperbranched copolymer aggregates. The acquired data are encouraging for the potential of these novel hyperbranched copolymers to be used as nanocarrier systems for medicinal applications.

Received 18th November 2022,
Accepted 28th December 2022

DOI: 10.1039/d2py01447e

rsc.li/polymers

Introduction

Hyperbranched copolymers and dendrimers belong to a well-known family of highly branched macromolecules with a three-dimensional dendritic-like architecture. Over the last few years, hyperbranched copolymers have gained the interest of polymer science and industry as well, due to their unique macromolecular topologies and remarkable physicochemical properties.[1–3] On the one hand, the multi-step synthesis of dendrimers requires repetitive purification steps, and thus, there are some limitations resulting in expensive materials in industry. On the other hand, the one-pot synthesis of randomly branched,[4,5] hyperbranched polymers makes them valuable and cost effective materials in large-scale industrial applications. In addition, hyperbranched copolymers presented several advantageous features in comparison with their linear analogues, including a large population of terminal functional groups, higher segment density, lower viscosity and better solubility.[6,7] Hyperbranched polymers compared to the corresponding linear polymers have the ability to self-assemble in more dense conformations in aqueous solutions.[8] These characteristics are attracting interest for a range of biomedical applications,[9] such as in drug[10–12] and gene delivery[13,14] and tissue engineering.[15,16]

In recent years, polymer-based nanomedicine has focused on functional polymeric materials that respond to physical and chemical stimuli such as temperature,[17–19] pH[20,21] and ionic strength.[22,23] These polymeric materials are frequently called "smart" polymers.[24] Several studies report on thermo-responsive polymers characterized by a low critical solution temperature (LCST) behavior.[25,26] In such cases below the LCST the polymeric system is completely miscible, with polymer chains being molecularly dissolved, whereas above the LCST partial liquid immiscibility occurs through the aggre-

Theoretical and Physical Chemistry Institute, National Hellenic Research Foundation, 48 Vassileos Constantinou Avenue, 11635 Athens, Greece. E-mail: pispas@eie.gr

† Electronic supplementary information (ESI) available. See DOI: https://doi.org/10.1039/d2py01447e

gation of polymeric chains as a result of the reduction of water–polymer interactions leading to the lower solubility of polymer chains. pH responsive polymeric systems are a category of responsive polymers that show changes in their conformation and aggregation state by changes in solution pH. Such copolymers contain in their chain monomers that consist of ionizable groups, and exhibit changes in their structural and physicochemical properties by altering the pH. The cationic polymers usually contain amino groups, such as poly (2-[dimethylamino]ethyl methacrylate) (PDMAEMA) and poly (2-[diisopropylamino]ethyl methacrylate) (PDIPAEMA) polymers,[27,28] where the protonation of amino groups transforms them into highly hydrophilic polymers when the solution pH is lower than the respective pK_a values of the basic pendant groups.

The synthesis of well-defined hyperbranched copolymers is achieved by controlled radical polymerization methods (ATRP,[29,30] NMP,[31,32] RAFT[33–35]), which show substantial compatibility with a wide range of monomers. Using RAFT polymerization, copolymers with predictable molecular weights, narrow molecular weight distributions, and different molecular architectures, *i.e.*, linear,[36,37] star,[38,39] and hyperbranched[40,41] copolymers, can be synthesized, whose properties in solution may be affected by temperature[42] and pH changes. A typical example of a thermoresponsive hyperbranched copolymer was reported by the Davis group. Utilizing RAFT polymerization, they synthesized a hyperbranched copolymer comprised of diethylene glycol methacrylate (DEGMA), oligo(ethylene glycol) methyl ether methacrylate (OEGMA, M_w = 475 g mol^{-1}) and the branching agent EGDMA. They studied the properties of hyperbranched copolymers in comparison with linear analogues. They found that the molecular architecture affected the thermoresponsive behavior, accompanied by a reduction of around 5–10 °C of the LCST of the hyperbranched copolymers in comparison with the LCST of the linear analogues.[43]

In the present study, we report on the one-step synthesis of three novel multi-responsive poly[(diethylene glycol methyl ether methacrylate)-*co*-(2-diisopropylamino ethyl methacrylate)], P(DEGMA-*co*-DIPAEMA), hyperbranched copolymers by the RAFT technique, in the presence of EGDMA as the branching agent. Furthermore, we studied the self-assembly behavior of the formed nanostructures in response to variations in physicochemical parameters such as temperature, pH and ionic strength, utilizing light scattering methods and fluorescence spectroscopy. Moreover, we studied the capability of these hyperbranched copolymers to encapsulate a hydrophobic drug, namely indomethacin (IND). Indomethacin is a non-steroidal anti-inflammatory drug commonly used as a prescription medication to reduce fever, pain, stiffness, and swelling from inflammation. Utilizing ultraviolet visible (UV-Vis) spectroscopy, it was possible to calculate the drug loading (%DL) and encapsulation efficiency (%EE). Finally, drug release profiles were obtained for the loaded hyperbranched copolymers at pH 7. From the point of view of hyperbranched copolymer design, the poly(diethylene glycol methyl ether methacrylate) (PDEGMA) homopolymer is a hydrophobic polymer above its T_{cp} (around 27 °C, molar mass dependent),[44] and becomes hydrophilic below the T_{cp}. Copolymers containing PDEGMA can be suitable candidates for a plethora of biomedical applications since the polymer is considered biocompatible.[45] The homopolymer of 2-(diisopropylamino)ethyl methacrylate (PDIPAEMA) is a dual-responsive polymer with regard to pH and temperature with a pK_a of around 6.2 [46] and a T_{cp} of *ca.* 27–60 °C.[47,48] PDIPAEMA is miscible with water as a cationic polyelectrolyte, due to the protonation of its amino groups close to below neutral pH and is transformed into a highly hydrophobic polymer at and above neutral pH, where deprotonation of the tertiary amine groups takes place. Based on the features mentioned above, we designed and synthesized these novel P(DEGMA-*co*-DIPAEMA) hyperbranched copolymers, having different compositions of the two thermoresponsive components, in order to explore the molecular structure–self-assembly property relationships in this new family of branched copolymers.

Experimental

Materials

The monomers diethylene glycol methyl ether methacrylate (DEGMA) (95%) and 2-(diisopropylamino)ethyl methacrylate (DIPAEMA) (97%), and the difunctional monomer/branching agent ethylene glycol dimethacrylate (EGDMA, 98%) were purchased from Sigma-Aldrich. The three monomers were passed through an inhibitor removing column for purification before polymerization (butylated hydroxytoluene and hydroquinone monomethyl ether inhibitor removers). 2,2′-Azobisisobutyronitrile (AIBN) was utilized as the radical initiator which was purified by recrystallization from methanol before use. 1,4-Dioxane (≥99.8% pure, Aldrich) was dried over molecular sieves before use. 4-Cyano-4-(phenylcarbonothioylthio)pentanoic acid (CPAD), tetrahydrofuran (THF 99.9% pure), *n*-hexane (≥97%), and other reagents were used as received.

Synthesis of P(DEGMA-*co*-DIPAEMA) hyperbranched copolymers

Dual-responsive hyperbranched copolymers were synthesized *via* reversible addition–fragmentation chain transfer (RAFT) polymerization of hydrophilic DEGMA (T_{cp} 28 °C), hydrophobic DIPAEMA (pK_a ~ 6.2) and EGDMA as the crosslinker/branching agent with relatively narrow molecular weight distributions ($M_w/M_n \leq 1.37$). AIBN and CPAD were utilized as a radical initiator and a chain transfer agent, respectively. 1,4-Dioxane was used as the solvent of the polymerization reaction. The P(DEGMA-*co*-DIPAEMA) hyperbranched copolymers which vary in composition will be referred to as HB-I, HB-II and HB-III in the order of increasing composition in DIPAEMA segments for brevity. A typical example of the synthetic process of a hyperbranched copolymer (HB-I) is described below: in a round-bottom flask (50 mL), DEGMA (1.45 g, 7.7 mmol), DIPAEMA (0.24 g, 1.12 mmol), EGDMA (0.032 g, 0.16 mmol), CPAD (0.048 g, 0.17 mmol), AIBN (0.0056 g,

0.03 mmol) and 1,4-dioxane (18 mL, 10% w/w monomer concentration) were added. The mixed solution was degassed under constant nitrogen gas flow for 20 min and then the round-bottom flask was placed in a pre-heated oil bath at 70 °C for 24 h. After the reaction, the mixture was placed at −20 °C followed by exposure to air to end the polymerization. Afterward, the product was precipitated two times in a large excess of *n*-hexane for the removal of unreacted monomers. Finally, the reaction product was placed for 48 h in a vacuum oven for drying at room temperature.

Self-assembly studies of dual-responsive hyperbranched copolymers in aqueous media

The self-assembly studies of hyperbranched copolymers were carried out in aqueous solutions prepared by the protocol described as follows: an appropriate quantity of solid polymer was dissolved directly in acidic water (10 mL), adjusted to pH 3, with an appropriate quantity of 0.1 M HCl (copolymer concentration, $c = 1 \times 10^{-3}$ g mL^{-1}) and the solutions were left overnight to equilibrate. Subsequently, appropriate quantities of 1 M NaOH solution were added to adjust the solution pH to 7 and 10. For fluorescence measurements, an appropriate quantity of pyrene probe solution (1 mM stock solution in acetone) was added to each P(DEGMA-*co*-DIPAEMA) hyperbranched copolymer solution of different pH values. All hyperbranched copolymer solutions were left overnight to bring the systems in equilibrium (final $c_{pyrene} = 10^{-7}$ M). The experiments on the effects of solution ionic strength were performed by increasing the solution salinity. An appropriate quantity of 1 M NaCl stock solution was added to the copolymer solution initially prepared. All stock solutions were filtered through 0.45 μm hydrophilic PVDF filters prior to measurements. Dynamic light scattering measurements were used to specify the changes in mass (*via* scattered intensity measurements) and the hydrodynamic radius R_h of copolymer solutions.

Preparation of IND-loaded P(DEGMA-*co*-DIPAEMA) nanocarriers

Indomethacin encapsulation into P(DEGMA-*co*-DIPAEMA) hyperbranched copolymers was performed *via* the thin film hydration method which is described below. First, two separate stock solutions of the copolymer in $CHCl_3$ and indomethacin in $CHCl_3$ were prepared. For the preparation of HB-I/10% w/w IND, 0.01 g of solid material and 0.18 g of IND were dissolved directly in an organic solvent. Afterwards, the solutions were mixed and placed in a spherical flask. By using a rotary evaporator the solvent was evaporated, leaving a thin copolymer/drug mixed film on the flask walls. Subsequently, a certain quantity of distilled water (10 mL) was added and gentle stirring at room temperature led to the formation of drug-loaded nanostructures in aqueous media. The entrapment of IND was successful only in two of the three copolymers, because the HB-III copolymer, due to its high composition of the hydrophobic DIPAEMA component was impossible to encapsulate and sustain a large amount of the drug (precipitates were visible within the solution after preparation). The IND-loaded copolymer nanoparticles were studied by DLS (at 25 °C and at 90° angle) to determine the structural properties of drug-loaded nanostructures. All drug-loaded copolymer solutions were filtered through 0.45 μm pore size filters and left overnight to bring the systems in equilibrium before measurements.

Drug loading and encapsulation efficiency of IND

Using UV-Vis spectroscopy it was possible to determine the actual percentage of drug encapsulated in the hyperbranched copolymer aggregates. The reference curve of indomethacin in $CHCl_3$ was constructed by measuring the absorbance at λ_{max} = 320 nm. %DL is the amount of drug loaded per unit mass of the drug/copolymer mixed assemblies, indicating the percentage of the mass of the nanoparticle that corresponds to the encapsulated drug. %DL can be calculated by the amount of total encapsulated drug divided by the total nanoparticle mass (drug + copolymer mass). %EE is the percentage of drug that is successfully encapsulated into the nanoparticle and is calculated by the mass of encapsulated drug divided by the total mass of the drug initially added.

$$\%\mathrm{DL} = [\text{mass of encapsulated drug/total nanoparticle mass}] \times 100 \quad (1)$$

$$\%\mathrm{EE} = [\text{mass of encapsulated drug/total drug mass added}] \times 100 \quad (2)$$

Drug release studies

The release of IND from HB-I and HB-II nanoassemblies was carried out at pH 7 by the dialysis method for approximately seven hours. In particular, 10 mL of IND loaded nanoparticles solution were added into a dialysis bag (MW cutoff 3500), which was placed in 10 times excess of distilled water. 3 mL of the external solution were taken at specific times and each time the aqueous media was restored to its initial volume, so that the conditions of the tank remained constant. The amount of IND released was evaluated by UV-Vis spectroscopy at λ_{max} = 320 nm.

Characterization methods

Size exclusion chromatography. The molecular weights and molecular weight distributions of the copolymers were determined by size exclusion chromatography, using a Waters instrument, consisting of a Waters 1515 isocratic pump, a set of three μ-Styragel mixed separation columns (pore range 10^2–10^6 Å), and a Waters 2414 refractive index detector (balanced at 40 °C) and controlled using Breeze software. The mobile phase was tetrahydrofuran, containing 5% v/v triethylamine, at a flow rate of 1 mL min^{-1}, and at 30 °C. Calibration of the instrument was performed using polystyrene standards with narrow molecular weight distributions and weight average molecular weights in the range of 2500 to 123 000 g mol^{-1}.

^{1}H-NMR spectroscopy. A Bruker AC 300 FT-R spectrometer was utilized for recording the ^{1}H-NMR spectra. The chemical shifts are recorded in parts per million (ppm) with reference to tetramethylsilane (TMS). For ^{1}H-NMR measurements, 10 mg of each copolymer were directly dissolved in 0.7 mL of deuterated chloroform before measurement and subsequently the copolymer solution was placed in NMR tubes. The spectra collection and analysis were accomplished using Mestre Nova software from Mestrelab.

^{1}H-NMR spectra peaks of P(DEGMA-*co*-DIPAEMA) (Fig. 2, 300 MHz, $CDCl_3$, ppm): 0.88, 1.23 (9H, –$CH_2C\mathit{CH}_3$–), 0.99 (3H, $CH_3\mathit{CH}$–), 1.6–2.28 (6H, –CH_2C–), 2.63 (2H, –$C\mathit{H}_2N$), 2.99 (H, –N$C\mathit{H}$), 3.38 (3H, O$C\mathit{H}_3$), 3.83, 4.09 ([(2H, –COO$\mathit{CH}_2(CH_2)$, 2H, –$COOCH_2(\mathit{CH}_2)$]].

UV-Vis spectroscopy. UV-Vis spectra were recorded using a PerkinElmer Lambda 19 UV-Vis spectrophotometer. 1 cm path quartz cells were utilized, placing each time 3 mL of the sample solution to be measured in the cell.

Fluorescence spectroscopy. Fluorescence measurements were recorded to determine the critical aggregation concentration (CAC) of the hyperbranched copolymers, using a NanoLog fluorometer (HORIBA Jobin Yvon). The instrument is equipped with a laser diode as the excitation source (Nano LED, 440 nm, 100 ps pulse width) and a UV TBX-PMT series detector (250–850 nm) from Horiba Jobin Yvon. Hyperbranched copolymer solutions were prepared at concentrations ranging from 10^{-8} to 10^{-3} g mL^{-1} and pyrene stock solution (1 mM) in acetone was added. The solutions were left overnight for the evaporation of acetone and to bring the systems in equilibrium and subsequently the I_1/I_3 ratio was measured at each polymer concentration (*i.e.*, the ratio of intensities of the first and the third vibronic peaks in the pyrene emission spectra). The excitation wavelength used for the measurements was 335 nm and emission spectra were recorded in the 355–640 nm region.

Light scattering. DLS measurements were accomplished utilizing an ALV/CGS-3 Compact Goniometer System (ALV GmbH, Germany), equipped with a JDS Uniphase 22 mW He–Ne laser operating at 632.8 nm, connected to a digital ALV-5000/EPP multi-tau correlator with 288 channels and an ALV/LSE-5003 light scattering module for step-by-step control of the goniometer and control of the end position switch. The instrument was connected to a Polyscience model 9102 bath circulator for temperature control of the measuring cell. The scattered light intensity and the correlation functions were recorded five times at each angle and concentration and analyzed by the cumulants method and the CONTIN algorithm. The latter provides the distributions of the apparent hydrodynamic radius (R_h), utilizing the Laplace inverse transform of the correlation function by employing the Stokes–Einstein relationship. Measurements at different temperatures were carried out in the 25 to 60 °C range, with 5 °C steps, allowing for 15 min equilibration between temperatures. The size data presented below correspond to measurements at an angle of 90°. All samples were filtered through 0.45 μm hydrophilic PVDF filters.

For static light scattering measurements the same instrument was utilized in the angular range of 30°–150° and at 25 °C. Toluene was used as the calibration standard. The dn/dc values were calculated from literature data (linear PDEGMA (dn/dc = 0.085 mL g^{-1}), those of linear POEGMA (dn/dc = 0.07 mL g^{-1}) and linear PDIPAEMA (dn/dc = 0.077 mL g^{-1}) were available, also based on the refractive indices of the constituting components and THF. Static light scattering profiles were analyzed by Zimm and Guinier models using the software available by the manufacturer.

Electrophoretic light scattering and ζ-potential. The ζ-potential was measured on a Malvern Nano Zeta Sizer system equipped with a He–Ne laser of 4 mW at a wavelength λ = 633 nm. It uses a photodiode as a detector and the scattered radiation is measured at an angle of 173°. Electrokinetic measurements to determine the mobility and ζp values of the colloids were performed using the LDV technique (Laser Doppler Velocimetry) and the Smoluchowski approximation. Reported ζp values are the mean of 100 measurements.

Results and discussion

P(DEGMA-*co*-DIPAEMA) hyperbranched copolymer synthesis and molecular characterization

A series of P(DEGMA-*co*-DIPAEMA) hyperbranched copolymers were synthesized *via* RAFT polymerization with different molecular characteristics. For the synthesis of all hyperbranched copolymers the EGDMA/CTA ratio was maintained constant at 1.1 to avoid gelation. The radical initiator AIBN was utilized for the synthesis of the hyperbranched copolymer as well as 1,4-dioxane as the solvent for the polymerization. The synthesis of P(DEGMA-*co*-DIPAEMA) copolymers was achieved at 70 °C for 24 h and the synthetic route is given in Scheme 1. CPAD was chosen as the chain transfer agent since it is suitable for methacrylate monomers as evidenced in the literature.[49] The choice of the EGDMA difunctional monomer as the crosslinker/branching agent resulted in the generation of the branched polymeric chains producing branching points. The molecular characterization of all hyperbranched copolymers was accomplished by means of SEC and ^{1}H-NMR techniques. A representative chromatogram of the HB-I copolymer is illustrated in Fig. 1. A narrow peak accompanied by symmetric molecular weight distribution and low dispersity is evident indicating control of the polymerization process. It should be mentioned that the molecular weights determined in the case of the branched copolymer by SEC are apparent ones because of the different hydrodynamic properties of the hyperbranched copolymers relative to the corresponding linear polystyrenes used for calibration. The molecular characteristics of all hyperbranched copolymers are presented in Table 1.

By utilizing ^{1}H-NMR spectroscopy the chemical structure and the composition of P(DEGMA-*co*-DIPAEMA) hyperbranched copolymers were determined. Characteristic peaks were selected to calculate the composition of each copolymer and are displayed in Fig. 2. For the DEGMA component the

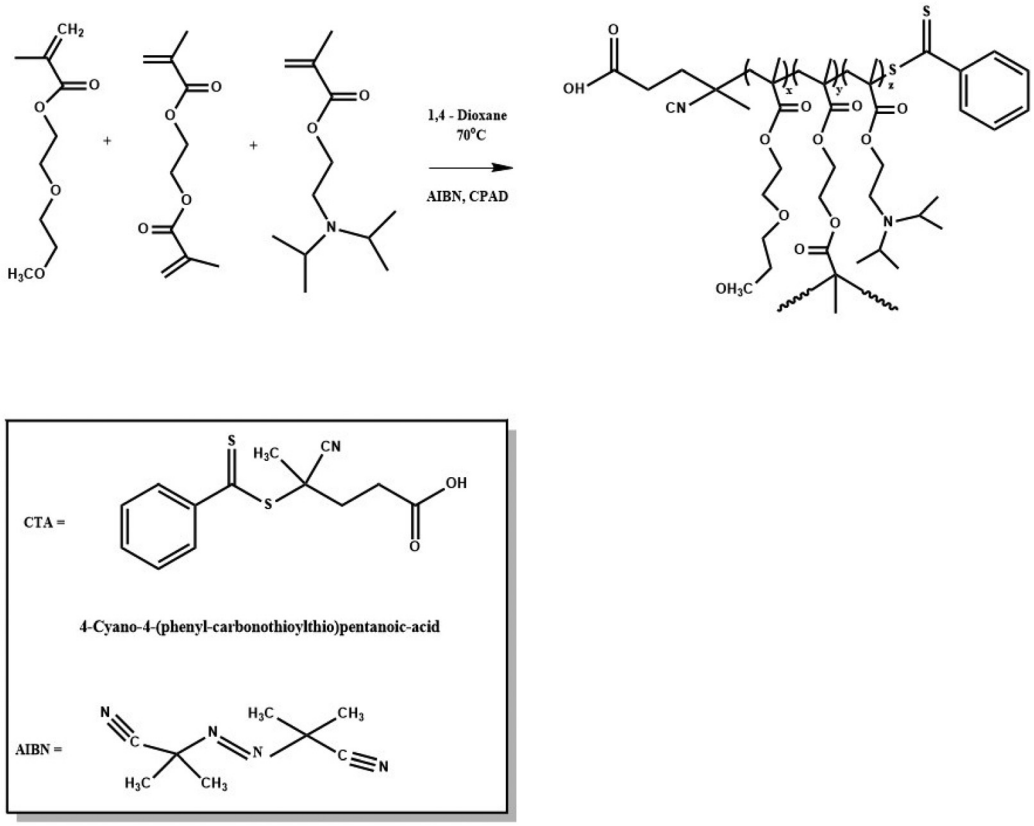

Scheme 1 Synthesis scheme followed for the preparation of P(DEGMA-*co*-DIPAEMA) hyperbranched copolymers.

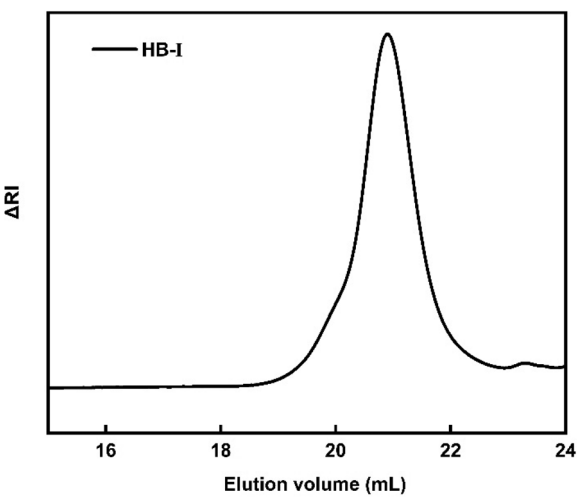

Fig. 1 SEC chromatogram of the HB-I hyperbranched copolymer.

$-CH_3$ protons at 3.38 ppm were chosen (peak f)[50] and for the PDIPAEMA the $-CH_2$ protons at 2.62 ppm were utilized (peak d).[28] It should be mentioned that the corresponding peak (g) of EGDMA is overlapped with the signals of the DEGMA peaks (h, z) at 3.61 ppm.

The apparent weight average molecular weights of the hyperbranched copolymers were determined by SLS measurements in THF measurements (a good solvent for all copolymer components). As shown from the results in Table 1, the $M_{w\ app}$ values acquired by SLS are higher than the M_w values obtained by SEC, supporting the hyperbranched macromolecular structure of the present copolymers.

Table 1 Molecular characteristics of P(DEGMA-*co*-DIPAEMA) hyperbranched copolymers

Sample	M_w $(10^4)^a$ (g mol^{-1})	$M_w/M_n{}^a$	M_w $(10^5)^b$ (g mol^{-1})	% wt DEGMA^c	% wt DIPAEMA^c
HB-I	0.98	1.18	3.09	82	18
HB-II	1.1	1.2	4.72	60	40
HB-III	1.2	1.22	3.61	46	54

[a] Determined by SEC. [b] Determined by SLS. [c] Determined by ^{1}H-NMR.

Self-assembly studies of hyperbranched copolymers in aqueous media

The composition and the hyperbranched architecture of P(DEGMA-*co*-DIPAEMA) copolymers are expected to affect the solution properties of the double hydrophilic hyperbranched copolymers, while various physicochemical stimuli can also affect the self-assembly state of these copolymers. An extensive study was undertaken, utilizing different physicochemical methods. Fluorescence spectroscopy was performed to evalu-

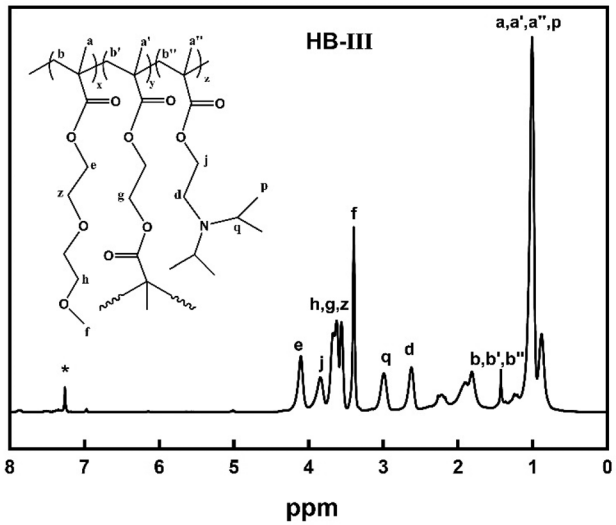

Fig. 2 ^{1}H-NMR spectrum of the HB-III hyperbranched copolymer.

ate the critical aggregation concentration (CAC) of the hyperbranched copolymers. In these experiments pyrene was used as the probe, since it is insoluble in water and has the ability to be localized in the hydrophobic domains of amphiphilic self-assembled nanoparticles formed in aqueous solutions. Specifically, I_1/I_3 represents the intensity ratio between the first and the third vibronic peaks in the pyrene fluorescence spectrum, which is highly sensitive to changes in the polarity of the probe microenvironment. The literature low values of the ratio I_1/I_3 (in the range of 1.0–1.3) represent the hydrophobic environment around pyrene. A more polar environment is revealed when the I_1/I_3 ratio has values in the range 1.7–1.9.[51] The copolymer solutions were prepared at concentrations ranging from 10^{-8} to 10^{-3} g mL^{-1}. Table 2 presents the I_1/I_3 values of the dual-responsive P(DEGMA-*co*-DIPAEMA) hyperbranched copolymers under different solution conditions regarding pH and temperature. CAC values are expected to be affected by changes in pH, temperature and the chemical composition of each copolymer in aqueous solutions. The measurements were recorded at pH 3, 7, and 10. At pH 3, no copolymer aggregates were observed, as evidenced by the high I_1/I_3 values, due to the hydrophilic character of DIPAEMA segments (fully protonated amino groups) at this pH, as DEGMA is also a hydrophilic component.[52] At pH 7 and pH 10 representative graphs of I_1/I_3 *vs.* copolymer concentration are illustrated in Fig. 3.

Table 2 I_1/I_3 values of P(DEGMA-*co*-DIPAEMA) hyperbranched copolymers as a function of pH and temperature ($c_{polymer}$ = 1 × 10^{-3} g mL^{-1})

		I_1/I_3	
Copolymer	pH	25 °C	55 °C
HB-I	3	1.58	1.49
	7	1.49	1.36
	10	1.35	1.24
HB-II	3	1.54	1.45
	7	1.38	1.32
	10	1.18	1.15
HB-III	3	1.57	1.47
	7	1.2	1.16
	10	1.14	1.1

In the plots shown above, a clear plateau is observed at low polymer concentrations, where there are no polymeric aggregates formed in aqueous media. The transition in the I_1/I_3 values between lower and higher copolymer concentrations revealed the formation of copolymer aggregates. Moreover, the chemical composition of each copolymer seems to affect the actual critical aggregation concentration, with the CAC switching to lower values for copolymer HB-III with the higher DIPAEMA content. The CAC always appears at lower concentrations at pH 10 and at higher concentrations at pH 7. This fact is to be expected since the closer to the neutral pH the more hydrophobic behavior is revealed by the copolymer, due to the partial or full deprotonation of the amino groups of DIPAEMA segments. Generally, the increased hydrophobicity of the DIPAEMA segments results in the formation of nanostructures at lower concentrations, especially at higher DIPAEMA contents. Table 2 presents the I_1/I_3 values of hyperbranched copolymers in aqueous solutions as a function of pH and temperature.

As shown in Table 2 above, the I_1/I_3 values demonstrate the microenvironment that pyrene experiences under each solution condition. The dual-responsive P(DEGMA-*co*-DIPAEMA hyperbranched copolymers exhibit a gamut of I_1/I_3 values under different physicochemical stimuli. Specifically, at pH 10 the full deprotonation of the amine groups of DIPAEMA segments leads to increased hydrophobicity of the copolymer, which is depicted by the reduction of I_1/I_3. Furthermore, at both extreme temperatures by increasing the amount of DIPAEMA component, the I_1/I_3 ratio seems to attain lower values. Interestingly by increasing the temperature the hydrophobicity of all copolymer systems is enhanced (at the same pH) which can be related to the thermo-responsiveness (LCST behavior with T_{cp} *ca.* 27 °C) of PDEGMA and the PDIPAEMA segments at higher temperatures (the I_1/I_3 ratio is smaller at 55 °C).

Taking into consideration the data presented above, the P(DEGMA-*co*-DIPAEMA) hyperbranched copolymers show amphiphilic character and self-assemble into polymeric aggregates, carrying hydrophobic domains, under the effect of temperature increase and pH-changes due to the thermo-response of PDEGMA and PDIPAEMA and the pH-response of PDIPAEMA components, modulated by the variable composition of each segment in the copolymer.

Additional studies of the dual-responsive P(DEGMA-*co*-DIPAEMA) hyperbranched copolymers in aqueous media were conducted by light scattering methods. The acquired results are presented in Table S1 (ESI).† In particular, by using the dynamic light scattering technique it was possible to evaluate several parameters such as the hydrodynamic radius (R_h) of the self-assembled polymeric aggregates, the changes in terms of the mass of nanoaggregates (*via* scattered intensity

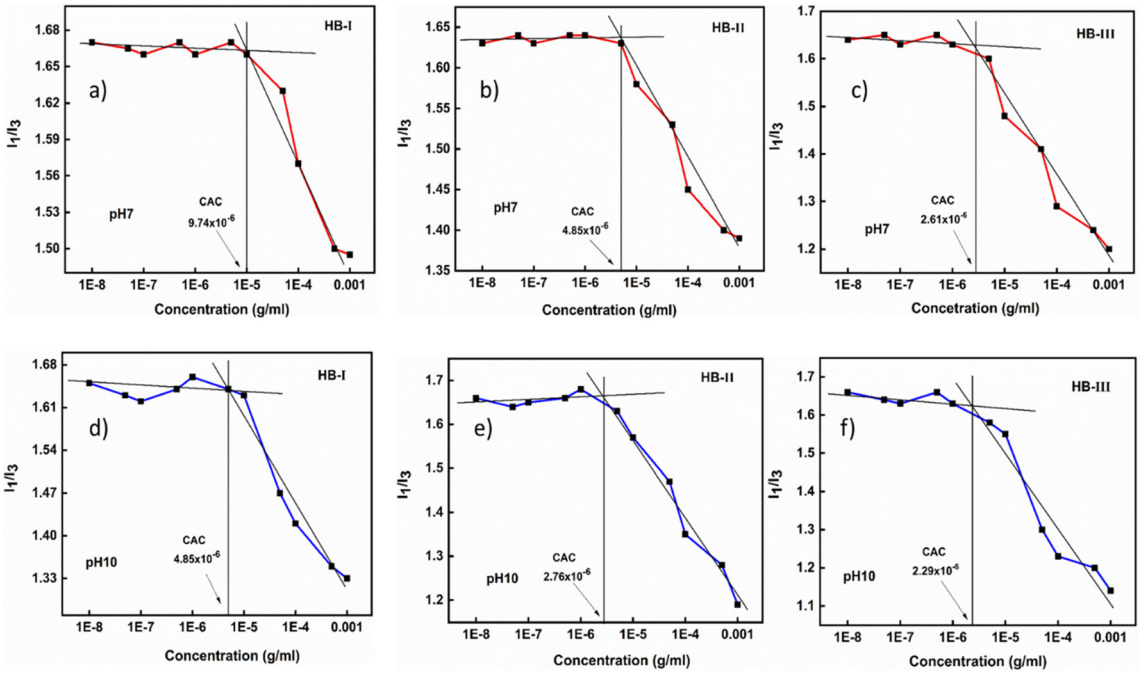

Fig. 3 CAC determination for P(DEGMA-*co*-DIPAEMA) hyperbranched copolymers at pH 7 (upper row: a, b and c) and pH 10 (lower row: d, e and f).

measurements) and their polydispersity index (PDI) due to temperature and pH alternations. Light scattering measurements for HB-I are presented in Fig. 4. Based on the Contin analysis results at 25 °C and 55 °C well-defined nanostructures were formed. Specifically, at pH 3 and at both temperatures, where the amino groups of PDIPAEMA are fully protonated and PDEGMA is in a hydrophobic state, nanoparticles of larger sizes are observed when they are compared to the other two pH values, probably due to the extended conformation of polymeric chains. Also, a narrow size distribution was observed at 55 °C in contrast to the lower temperature (PDI = 0.45 at 25 °C *vs.* PDI = 0.12 at 55 °C). At pH 10 and at both temperatures, the full deprotonation of PDIPAEMA chains and the hydrophobic character of PDEGMA lead to a reduction in the dimensions of the formed polymeric aggregates. At this pH value both components are in their most hydrophobic state, resulting in the formation of compact nanoparticles showing narrow size distributions. An interesting observation takes place at pH

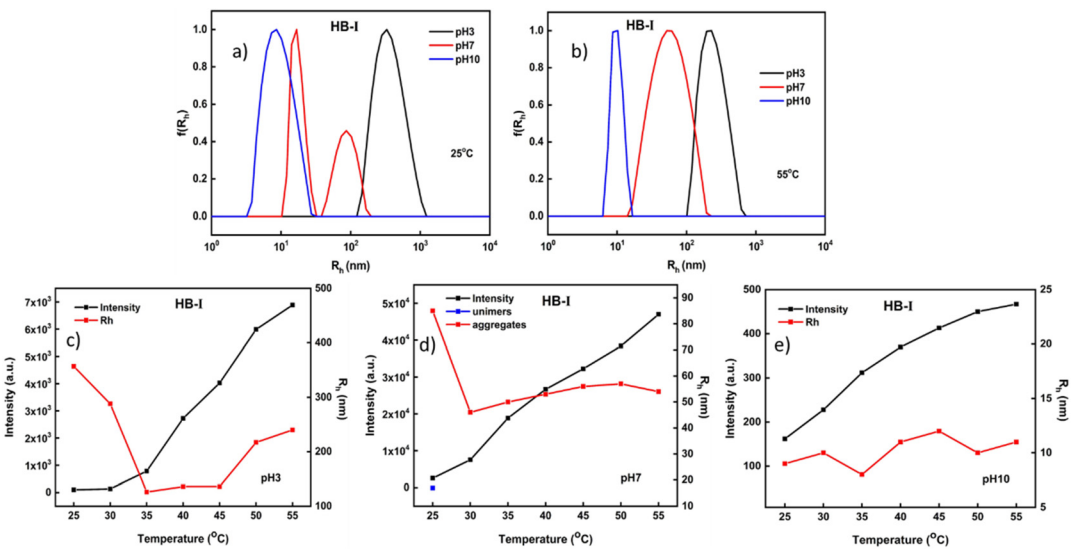

Fig. 4 Light scattering results for the HB-I hyperbranched copolymer solutions: size distributions from DLS (upper row: a and b) and variation of the scattered intensity and R_h as a function of pH and temperature (lower row: c, d and e).

7 in comparison with lower and higher temperatures. In particular, at this pH and at a lower temperature (Fig. 4a), the partial deprotonation of DIPAEMA chains led to the formation of two populations. The opposite is observed at a higher temperature (Fig. 4b), where both copolymer components impart sufficient hydrophobicity to the system, resulting in the formation of better-defined nanostructures.

Furthermore, studies were carried out to evaluate the changes in scattered intensity (*i.e.*, the changes in the mass of the nanoparticles) as a function of pH and temperature. As shown in the characteristic graphs below, an increase in scattered intensity is observed at all pH values. At pH 3 and 25 °C both PDEGMA and PDIPAEMA elements are in the most well-solvated state (Fig. 4c). By increasing the temperature, the mass of the self-organized nanoparticles formed in aqueous media increases as the PDEGMA component shifts to a more hydrophobic state. Also, the nanoparticles have the tendency to reduce their initial sizes as both constituents are in the hydrophobic form but as temperature increases some small variation is observed (Fig. 4c). At pH 7 there are interesting differences in the mass and dimensions of the aggregates compared to pH 3. The amino groups of PDIPAEMA are partially protonated here giving a more hydrophobic character to the system, and this is demonstrated by the *ca.* 25 times rise in mass, accompanied by an almost 3.5 times reduction in the size of the nanoparticles in comparison with acidic conditions. Also, it seems that the temperature has no significant effect on the sizes of the nanoparticles at pH 7. At pH 10 where the DIPAEMA segments are fully deprotonated, the formation of nanoparticles of low mass accompanied by small sizes is observed. It appears that at pH 10 the strong hydrophobicity of DIPAEMA significantly affects the system, in combination with the hydrophobicity presented by PDEGMA as temperature increases. At 55 °C, DEGMA chains are in the most hydrophobic conditions and in a more compact conformation. This combination leads to the formation of nanoparticles of small sizes and masses with fairly well-defined overall structures.

Fig. 5 presents the light scattering results from HB-III copolymer solutions. This hyperbranched copolymer has the larger PDIPAEMA content. The high content of PDIPAEMA most probably allows the polymeric system to be organized in more swollen (loose) aggregates with relatively wide size distributions under acidic conditions. A fairly narrow size distribution is observed at pH 10 in both temperatures, where DIPAEMA chains are fully deprotonated leading to a more compact aggregate structure. It is speculated that this occurs because of the greater content of DIPAEMA which gives the system an extra impetus to form well-defined nanostructures. It appears that by decreasing the PDEGMA content, at higher temperatures, the nanoparticles formed have more extended structures and relatively broader size distributions. The opposite has been observed in the case of the HB-I copolymer, where the dominant component is DEGMA.

Based on the changes in the mass and sizes of the nanoaggregates, several interesting observations can be made. By increasing pH, a remarkable increase in the mass of the formed nanoparticles is observed. This is due to the high content in PDIPAEMA which enhances the hydrophobicity of the polymeric system and its subsequent aggregation. At pH 3 the thermal response of both components leads to a reduction of the scattering intensity (mass). The opposite happens in the case of HB-I which consists primarily of DEGMA (Fig. 4c). Regarding the dimensions of the nanoparticles, it seems that when the temperature increases there is a relative reduction in the aggregate sizes which, however, return to their initial values at higher temperatures (Fig. 5c). At pH 7 a linear

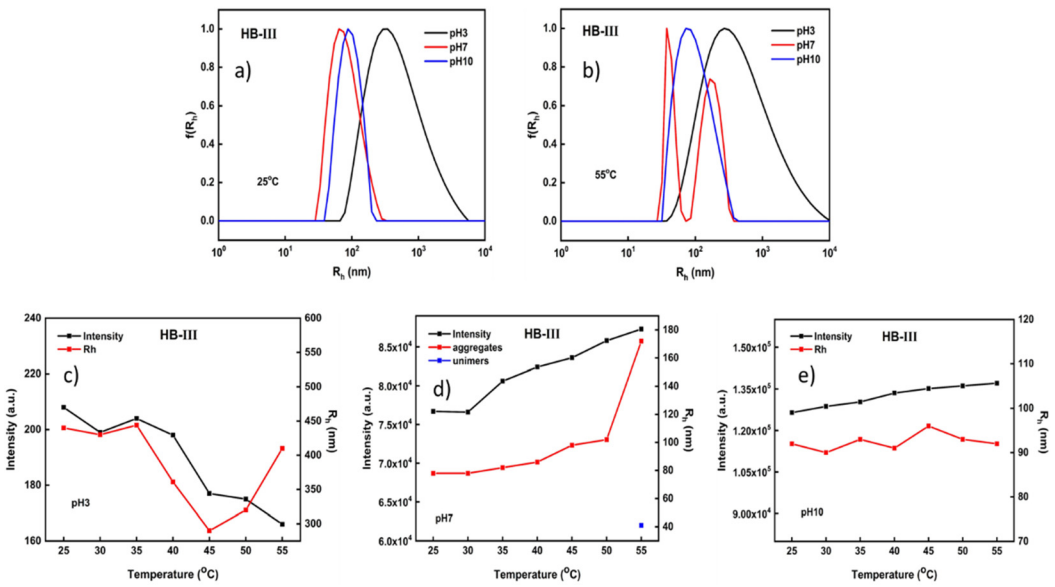

Fig. 5 Light scattering results for the HB-III hyperbranched copolymer solutions: size distributions from DLS (upper row: a and b) and variation of the scattered intensity and R_h as a function of pH and temperature (lower row: c, d and e).

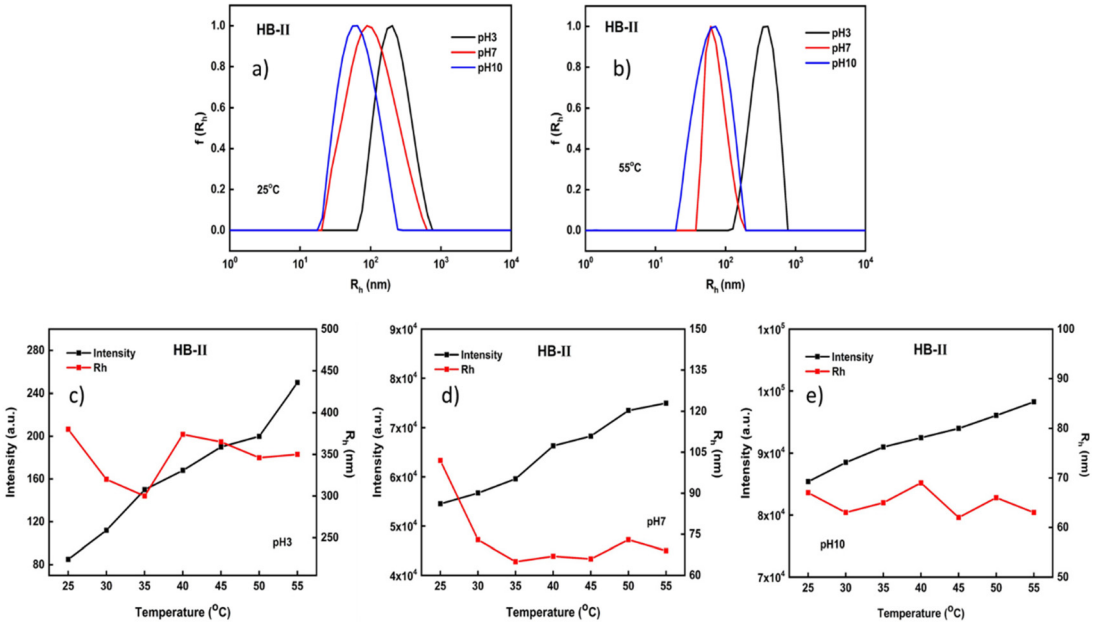

Fig. 6 Light scattering results for the HB-II hyperbranched copolymer solutions: size distributions from DLS (upper row: a and b) and variation of the scattered intensity and R_h as a function of pH and temperature (lower row: c, d and e).

increase in the scattered intensity and dimensions of the nanoparticles occurs by increasing the temperature, except for the transition between 50 °C and 55 °C, where there is a sharp increase of the sizes (almost 2 times). At pH 10 no significant changes are observed in the mass or sizes of the aggregates *vs.* temperature. As mentioned above, this copolymer at pH 10 tends to form more dense and well-defined structures across a wide range of temperatures.

Light scattering measurements for the HB-II copolymer are illustrated in Fig. 6. This polymer is in an intermediate condition in comparison with the other two polymeric systems in terms of its composition. Considering the plots given below, at 25 °C it appears that nanoparticles with relatively broad size distributions were formed at all pH values. Interestingly by changing the pH or temperature there was no second nanoparticle population observed. In practice, the sizes observed had intermediate values in comparison to the other two copolymers at all ranges of pH and temperature (see also the results in the ESI†). This may be due to the fact that the system has a more balanced monomer composition even though PDEGMA slightly predominates. As described above (see the behavior of HB-I), when DEGMA was dominant two populations appeared at 25 °C and at pH 7 (Fig. 4a), where at this temperature PDEGMA is close to its LCST. Furthermore, in the case of the HB-III copolymer, where DIPAEMA predominates, two populations of nanoparticles were formed at pH 7 and 55 °C (Fig. 5b). Under these conditions PDIPAEMA is quite hydrophobic since it is above its pK_a and its LCST.

Based on the changes in the mass of the formed aggregates in the case of HB-II, the same pattern is observed at all pH values. In particular, as the pH increases, an increase in scattered intensity is observed. Interestingly, in the case of HB-II aggregates, as the pH increases, a reduction in size is evident. As mentioned above, when PDIPAEMA is above its pK_a, its amino groups are partially or fully deprotonated converting it to a hydrophobic polymer. Therefore, there are no particular changes in the size of the formed nanoparticles at all pH values by increasing the temperature.

Effect of solution ionic strength on hyperbranched P(DEGMA-*co*-DIPAEMA) self-assembly

The P(DEGMA-*co*-DIPAEMA) hyperbranched copolymers under acidic conditions are fully protonated, and thus are converted to hyperbranched polyelectrolytes. Taking that into account, the impact of solution ionic strength on the structural changes of the polymeric aggregates formed was investigated. Characteristic plots showing changes in the size and mass of polymeric assemblies as a function of NaCl concentration in aqueous media are illustrated in Fig. 7.

An increase of salt concentration reveals a gradual increase in the mass of polymeric aggregates in all hyperbranched copolymer solutions. In particular, as the DIPAEMA component in the copolymer increases, the mass of nanoparticles shows higher values at a higher NaCl concentration. In the case of HB-III, the largest values regarding the dimension of the formed nanoparticles are observed. In an acidic environment, the HB-III copolymer shows the highest ζ-potential values (because of the highest DIPAEMA content), resulting in the formation of nanoparticles of larger dimensions compared to the other two copolymers. This is due to the high concentration of protonated (positively charged) amino groups which are affected by the NaCl concentration increase. In the case of

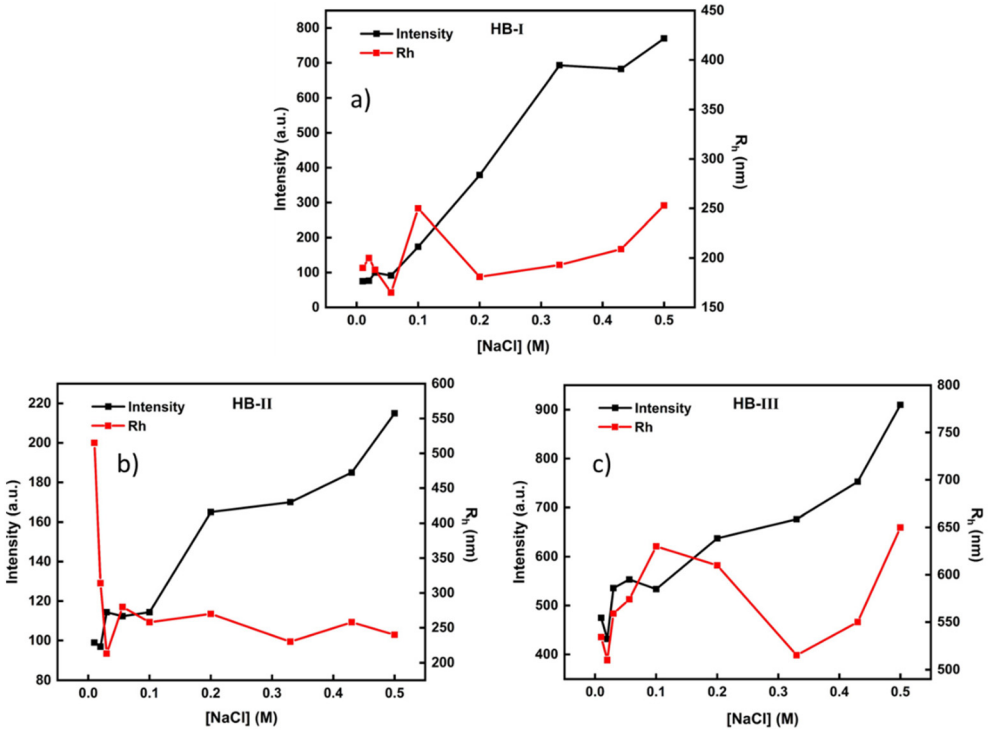

Fig. 7 Light scattering measurements for P(DEGMA-*co*-DIPAEMA) hyperbranched copolymer solutions (c = 1 × 10^{-3} g mL^{-1}) at pH 3 as a function of solution ionic strength. (a) HB-I, (b) HB-II, (c) HB-III.

HB-I no significant changes in particle dimensions are observed with changes in solution ionic strength. This may be due to the low PDIPAEMA content of the particular copolymer. In the case of HB-II, a sharp increase in the dimensions of the self-assembled nanoparticles occurs by the first addition of NaCl in the solution, where subsequent additions of salt create a plateau in terms of aggregate dimensions. This may be a result of the screening effects of salt on the positively charged amino groups.

Indomethacin loading to P(DEGMA-*co*-DIPAEMA) hyperbranched copolymers

The ability of P(DEGMA-*co*-DIPAEMA) hyperbranched copolymers to act as drug vehicles was investigated next. Indomethacin (IND) was utilized as a model hydrophobic drug, which was able to be entrapped into the hydrophobic domains of copolymer aggregates. The properties of the drug-loaded polymeric aggregates were determined by dynamic light scattering (DLS) and ultraviolet visible spectroscopy (UV-Vis). The encapsulation of IND was accomplished according to the protocol described in the experimental part. In the case of HB-II only 10% w/w of IND was able to be encapsulated. This should be related to the high PDIPAEMA content. The high amount of hydrophobic component, in combination with the high concentration of the hydrophobic drug, creates an imbalance in the mixed copolymer–drug system. This results in the precipitation of the drug or disintegration of mixed copolymer/drug nanoparticles. The final concentration of the copolymer solutions was 1 × 10^{-3} g mL^{-1}. DLS measurements were recorded at 25 °C and 90° angle. UV-Vis was used to specify the successful encapsulation of indomethacin in the polymeric aggregates, which are reported in the ESI.† By using the calibration curve of indomethacin in chloroform, the actual quantity of the encapsulated drug was calculated, which is reported in Table S2.† Fig. 8 shows the comparative plots of size distributions, before and after indomethacin encapsulation.

Fig. 8 depicts the remarkable differences in the size distributions between the neat and drug-loaded hyperbranched nanoparticles. In the case of the IND-loaded HB-I copolymer, it is observed that the encapsulation of the IND enhanced the self-assembly of polymeric aggregates. Specifically, one population of particles is present which demonstrates more well-defined nanostructures with the addition of the drug. Furthermore, as the amount of loaded drug increases, the sizes of loaded copolymer nanoparticles appear to decrease. This is likely to be due to the hydrophobic interactions between the polymer and the drug, which lead to more efficient entrapment of the drug in the hydrophobic domains of polymeric aggregates and also shrinkage of the mixed copolymer–drug nanoparticles which are now becoming more hydrophobic in nature. The same pattern seems to be followed by the other hyperbranched copolymer HB-II. It is worth mentioning that a gradual increase in the mass of IND-loaded polymeric aggregates occurs (Table 3), which indicates the more efficient formation of loaded copolymer nanoassemblies by

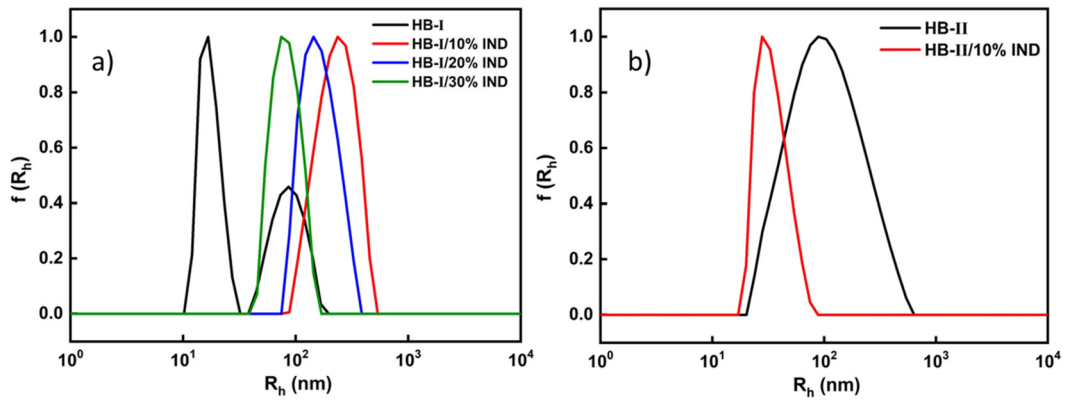

Fig. 8 Comparative plots of size distributions from DLS for P(DEGMA-*co*-DIPAEMA) hyperbranched solutions before and after encapsulation of indomethacin. (a) bare/loaded-HB-I copolymer, (b) bare/loaded-HB-II copolymer.

Table 3 DLS measurements for bare and IND-loaded hyperbranched nanoparticles

		Intensity[a] (kHz)		R_h [a] (nm)		PDI[a]	
Sample	%IND	With IND	Without IND	With IND	Without IND	With IND	Without IND
HB-I	10	2.477	2.547	226	17/85	0.4	0.36
	20	5.567	2.547	160	17/85	0.43	0.36
	30	42.400	2.547	82	17/85	0.3	0.36
HB-II	10	1.941	54.000	66	102	0.41	0.4

[a] By DLS at an angle of 90°.

the incorporation of hydrophobic indomethacin in the mixed system.

Drug release profiles from the hyperbranched copolymer aggregates

IND-loaded hyperbranched copolymer mixed aggregates were studied in order to evaluate the drug release. Fig. 9 presents the cumulative drug release *vs.* time for both nanocarrier systems. Drug release studies reveal that both nanocarriers were able to release IND. Specifically, it appears that in the first 50 min both polymeric systems release about the same amount of drug. Then HB-II seems to release a higher amount of drug, which may be attributed to the composition of the copolymer and the overall structure of the mixed drug–copolymer aggregates. In particular, as mentioned above at pH 7 the DIPAEMA segments are partially protonated, and in combination with a higher DIPAEMA content in the HB-II copolymer, this may lead to a more effective release of the drug.

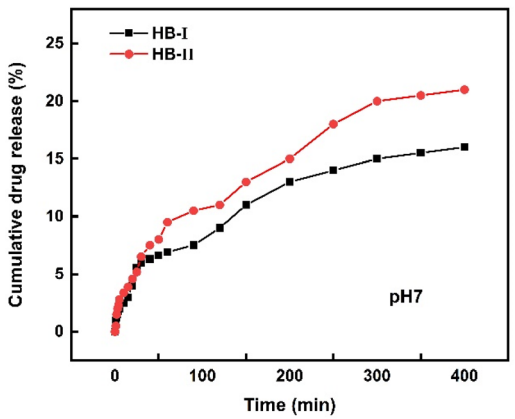

Fig. 9 Drug release from IND-loaded hyperbranched copolymer nanoassemblies in pH 7 solutions.

Conclusions

A novel series of temperature and pH-responsive P(DEGMA-*co*-DIPAEMA) hyperbranched copolymers were synthesized *via* RAFT polymerization using EGDMA as the branching agent. Results from static light scattering together with SEC experiments supported the hyperbranched molecular architecture of the newly synthesized copolymers. The hyperbranched copolymer self-assembled nanostructures formed in aqueous media were found to be responsive to temperature and pH. Fluorescence spectroscopy using pyrene as the probe showed the dependence of CAC values of the copolymer aggregates on pH and temperature. Structural characteristics of the aggregates are strongly dependent on the copolymer composition. With the aid of light scattering measurements, the aggregates were found to increase in mass as the solution temperature increased. When DIPAEMA segments were fully deprotonated, nanostructures of small dimensions were observed.

Furthermore, when DEGMA predominates as a component in the copolymer, nanoparticles with more well-defined structures were formed. Additionally, experiments as a function of solution ionic strength showed that larger polymeric aggregates are formed by increasing the NaCl concentration. Indomethacin encapsulation increased the hydrophobic character of the mixed aggregates and rather well-defined nanostructures were formed with a higher mass and size, but within nanoscale dimensions. Moreover, drug release profiles exhibited low release rates, which indicates that a high amount of the entrapped IND is strongly attached to the hydrophobic domains of the hyperbranched copolymer aggregates. The stimuli responsive amphiphilic character and structural flexibility of these new hyperbranched copolymers may be useful for their utilization as drug nanocarriers and as functional nanostructures and nanomaterials in other nanotechnological applications.

Conflicts of interest

There are no conflicts to declare.

References

1 F. Wurm and H. Frey, *Prog. Polym. Sci.*, 2011, **36**, 1–52.
2 D. Wang, T. Zhao, X. Zhu, D. Yan and W. Wang, *Chem. Soc. Rev.*, 2015, **44**, 4023–4071.
3 N. M. Smeets, *Eur. Polym. J.*, 2013, **49**, 2528–2544.
4 D. Wilms, M. Schömer, F. Wurm, M. I. Hermanns, C. J. Kirkpatrick and H. Frey, *Macromol. Rapid Commun.*, 2010, **31**, 1811–1815.
5 A. Balafouti and S. Pispas, *J. Polym. Sci.*, 2022, **60**(13), 1931–1943.
6 Y. Segawa, T. Higashihara and M. Ueda, *Polym. Chem.*, 2013, **4**, 1746–1759.
7 D. Zhang, D. Jia and Z. Zhou, *Macromol. Res.*, 2009, **17**, 289–295.
8 G. C. Behera, A. Saha and S. Ramakrishnan, *Macromolecules*, 2005, **38**, 7695–7701.
9 Y. Zhou, W. Huang, J. Liu, X. Zhu and D. Yan, *Adv. Mater.*, 2010, **22**, 4567–4590.
10 D. Wang, H. Chen, Y. Su, F. Qiu, L. Zhu, X. Huan, B. Zhu, D. Yan, F. Guo and X. Zhu, *Polym. Chem.*, 2013, **4**, 85–94.
11 S. Lee, K. Saito, H.-R. Lee, M. J. Lee, Y. Shibasaki, Y. Oishi and B.-S. Kim, *Biomacromolecules*, 2012, **13**, 1190–1196.
12 D. Selianitis, A. Forys, B. Trzebicka, A. Alemayehu, V. Tyrpekl and S. Pispas, *Nanomanufacturing*, 2022, **2**, 53–68.
13 S. Chen, S. X. Cheng and R. X. Zhuo, *Macromol. Biosci.*, 2011, **11**, 576–589.
14 Y. Nakayama, *Acc. Chem. Res.*, 2012, **45**, 994–1004.
15 M. Xie, L. Wang, B. Guo, Z. Wang, Y. E. Chen and P. X. Ma, *Biomaterials*, 2015, **71**, 158–167.
16 A. Saadati, M. Hasanzadeh and F. Seidi, *TrAC, Trends Anal. Chem.*, 2021, **142**, 116308.
17 A. Ramírez-Jiménez, K. A. Montoya-Villegas, A. Licea-Claverie and M. A. Gónzalez-Ayón, *Polymers*, 2019, **11**, 1657.
18 Y. Wang, Y. Kotsuchibashi, Y. Liu and R. Narain, *Langmuir*, 2014, **30**, 2360–2368.
19 J. Yan, X. Zhang, W. Li, X. Zhang, K. Liu, P. Wu and A. Zhang, *Soft Matter*, 2012, **8**, 6371–6377.
20 S. J. T. Rezaei, H. S. Abandansari, M. R. Nabid and H. Niknejad, *J. Colloid Interface Sci.*, 2014, **425**, 27–35.
21 D.-B. Cheng, P.-P. Yang, Y. Cong, F.-H. Liu, Z.-Y. Qiao and H. Wang, *Polym. Chem.*, 2017, **8**, 2462–2471.
22 S. Saliba, C. Valverde Serrano, J. Keilitz, M. L. Kahn, C. Mingotaud, R. Haag and J.-D. Marty, *Chem. Mater.*, 2010, **22**, 6301–6309.
23 X. Liu, H. Li, Z. Xu, J. Peng, S. Zhu and H. Zhang, *Anal. Chim. Acta*, 2013, **797**, 40–49.
24 D. Wang, Y. Jin, X. Zhu and D. Yan, *Prog. Polym. Sci.*, 2017, **64**, 114–153.
25 Y. Kotsuchibashi, M. Ebara, T. Aoyagi and R. Narain, *Polymers*, 2016, **8**, 380.
26 A. P. Constantinou, L. Wang, S. Wang and T. K. Georgiou, *Polym. Chem.*, 2023, DOI: **10.1039/D2PY01097F**.
27 A. Skandalis and S. Pispas, *Polym. Chem.*, 2017, **8**, 4538–4547.
28 D. Selianitis and S. Pispas, *J. Polym. Sci.*, 2020, **58**, 1867–1880.
29 R. Qiang, G. Fanghong, J. Bibiao, Z. Dongliang, F. Jianbo and G. Fudi, *Polymer*, 2006, **47**, 3382–3389.
30 J. Han, S. Li, A. Tang and C. Gao, *Macromolecules*, 2012, **45**, 4966–4977.
31 S. Peleshanko, R. Gunawidjaja, S. Petrash and V. Tsukruk, *Macromolecules*, 2006, **39**, 4756–4766.
32 X. Wang and H. Gao, *Polymers*, 2017, **9**, 188.
33 A. P. Vogt, S. R. Gondi and B. S. Sumerlin, *Aust. J. Chem.*, 2007, **60**, 396–399.
34 B. Liu, A. Kazlauciunas, J. T. Guthrie and S. Perrier, *Macromolecules*, 2005, **38**, 2131–2136.
35 G. Liu, Q. Qiu and Z. An, *Polym. Chem.*, 2012, **3**, 504–513.
36 A. Skandalis, T. Sentoukas, D. Giaouzi, M. Kafetzi and S. Pispas, *Polymers*, 2021, **13**, 1698.
37 D. Selianitis and S. Pispas, *Polym. Int.*, 2021, **70**, 1508–1522.
38 E. Vlassi, A. Papagiannopoulos and S. Pispas, *J. Polym. Sci.*, 2021, **59**, 775–786.
39 C. Bray, R. Peltier, H. Kim, A. Mastrangelo and S. Perrier, *Polym. Chem.*, 2017, **8**, 5513–5524.
40 H. Tai, C. L. Duvall, A. S. Hoffman, P. S. Stayton and W. Wang, *Macromol. Mater. Eng.*, 2012, **297**, 1175–1183.
41 X. Zhou, J. Zhu, M. Xing, Z. Zhang, Z. Cheng, N. Zhou and X. Zhu, *Eur. Polym. J.*, 2011, **47**, 1912–1922.
42 P. De and B. S. Sumerlin, *Macromol. Chem. Phys.*, 2013, **214**, 272–279.
43 M. Luzon, C. Boyer, C. Peinado, T. Corrales, M. Whittaker, L. Tao and T. P. Davis, *J. Polym. Sci., Part A: Polym. Chem.*, 2010, **48**, 2783–2792.

44 C. Pietsch, U. S. Schubert and R. Hoogenboom, *Chem. Commun.*, 2011, **47**, 8750–8765.
45 K. Sun, M. Xu, K. Zhou, H. Nie, J. Quan and L. Zhu, *Mater. Sci. Eng., C*, 2016, **68**, 172–176.
46 Y. Q. Hu, M. S. Kim, B. S. Kim and D. S. Lee, *Polymer*, 2007, **48**, 3437–3443.
47 T. Thavanesan, C. Herbert and F. A. Plamper, *Langmuir*, 2014, **30**, 5609–5619.
48 B. Pang, Y. Yu and W. Zhang, *Macromol. Rapid Commun.*, 2021, **42**, 2100504.
49 J. Coupris, S. Pascual, L. Fontaine, T. Lequeux and T. N. Pham, *Polym. Chem.*, 2015, **6**, 4597–4604.
50 N. P. Truong, M. R. Whittaker, A. Anastasaki, D. M. Haddleton, J. F. Quinn and T. P. Davis, *Polym. Chem.*, 2016, **7**, 430–440.
51 M. Wilhelm, C. L. Zhao, Y. Wang, R. Xu, M. A. Winnik, J. L. Mura, G. Riess and M. D. Croucher, *Macromolecules*, 1991, **24**, 1033–1040.
52 X. Xu, A. E. Smith, S. E. Kirkland and C. L. McCormick, *Macromolecules*, 2008, **41**, 8429–8435.